Finite Elements in Analysis and Design 47 (2011) 1146–1156

Contents lists available at ScienceDirect

Finite Elements in Analysis and Design

journal homepage: www.elsevier.com/locate/finel

Complex variable methods for shape sensitivity of finite element models

Andrew Voorhees, Harry Millwater*, Ronald Bagley

University of Texas at San Antonio, San Antonio, TX 78249, USA

ARTICLE INFO

Article history:
Received 25 November 2010
Received in revised form
4 May 2011
Accepted 9 May 2011
Available online 2 June 2011

Keywords:
Design sensitivities
Optimization
Sensitivity methods
Complex Taylor series expansion (CTSE)
Finite differencing
Fourier differentiation

ABSTRACT

Shape sensitivity analysis of finite element models is useful for structural optimization and design modifications. Complex variable methods for shape sensitivity analysis have some potential advantages over other methods. In particular, for first order sensitivities using the complex Taylor series expansion method (CTSE), the implementation is straightforward, only requiring a perturbation of the finite element mesh along the imaginary axis. That is, the real valued coordinates of the mesh are unaltered and no other modifications to the software are required. Fourier differentiation (FD) provides higher order sensitivities by conducting an FFT analysis of multiple complex variable analyses around a sampling radius in the complex plane. Implementation of complex variable sensitivity methods requires complex variable finite element software such that complex nodal coordinates can be used to implement a perturbation in the shape of interest in the complex domain. All resulting finite element outputs such as displacements, strains and stresses become complex and accurate derivatives of all finite element outputs with respect to the shape parameter of interest are available. The methodologies are demonstrated using two-dimensional finite element models of linear elasticity problems with known analytical solutions. It is found that the error in the sensitivities is primarily defined by the error in the finite element solution not the error in the sensitivity method. Hence, more accurate sensitivities can be obtained through mesh refinement.

1. Introduction

Finite element analysis (FEA) is a powerful general-purpose tool in computational engineering that allows for the approximate solution of nonlinear boundary value partial differential equations defined on complicated and intricate domains with arbitrary boundary conditions [1]. As a result, FEA has become an essential part of the design process in science and engineering.

Design sensitivity analysis encompasses the development and computation of the sensitivities (partial derivatives) of the finite element (FE) output quantities with respect to parameters of interest contained in the FE model. Design sensitivities quantify the effect that a small design change has on the performance of the model and allow identification of important variables and effective optimizations to be carried out [2]. In addition, sensitivities are useful in other fields such as when using the first order reliability method in probabilistic analysis [3].

Shape sensitivity analysis encompasses the partial derivative of the model output with respect to a geometric shape, i.e., an underlying shape of the part, e.g., hole radius, curvature of an arch [4], wing shape design variables [5], crack length [6], and many others. Several methods exist for determining design sensitivities including finite differencing methods, equation-based methods, code-based methods, and complex variable sensitivity methods.

Finite differencing is the simplest and most straightforward method to obtain sensitivities as no coding modifications are required, and the method can be performed using commercial software without alteration. The sensitivity is estimated by perturbing the variable of interest, rerunning the analysis, and taking the difference in the function's output divided by the amount of the perturbation. Although simple in concept, finite differencing has several inadequacies. In particular, the accuracy may be poor as the method requires the subtraction of two near-equal numbers; hence the size of the perturbation (neither too large or too small) becomes critical. Second, implementing a perturbation of a shape design variable with a finite element mesh is problematic as mesh distortion issues must be addressed. As a result, alternative methods have been developed.

One alternative approach to finite differencing is to derive equations that represent the sensitivities and then solve these equations using the same techniques used to solve the original problem. These methods can be referred to as equation-based methods since the sensitivities are derived directly from the numerical model [7]. There are two basic methods by which the sensitivity equations can be obtained. The first of these two methods, direct differentiation, computes the sensitivities

* Corresponding author. Tel.: +1 210 458 4481; fax: +1 210 458 6504.
E-mail address: harry.millwater@utsa.edu (H. Millwater).

0168-874X/$ - see front matter © 2011 Elsevier B.V. All rights reserved.
doi:10.1016/j.finel.2011.05.003

through the differentiation of the governing equations analytically using the chain rule and solving the auxiliary equations in addition to the traditional equations [8]. First order [9] and second order [10,11] formulations have been developed. Derivations have been implemented for static and time dependent linear and nonlinear structural systems. The second method is called the adjoint method. This method can be thought of as the reverse of direct differentiation in that the formulations are derived by working from the outputs rather than the inputs using the calculus of variations [7,8]. The benefit of the adjoint method as opposed to the direct method is that it is computationally more efficient for problems with many inputs and few outputs. Although accurate and convenient once implemented, equation-based methods require a lengthy derivation of the governing equations with respect to nodal coordinates and subsequent computer implementation. Thus, the "cost of entry" to use equation-based methods is high.

Code-based methods are based on the same mathematics as equation based methods; however, the sensitivities are derived from the numerical solution rather than from the governing equations [7]. While code-based methods can be derived manually, one immediate benefit is that the process can be automated and carried out by a computer, referred to as automatic differentiation. Automatic differentiation is based on the concept of the chain rule and the fact that a large code thought of as a single function is composed of multiple smaller functions each having its own partial derivative [12]. By tracking the use of each smaller function, i.e. every multiplication or subtraction operation, and storing the derivative information, sensitivities can be obtained by applying the chain rule. The derivatives can be computed through both direct differentiation (often called forward mode differentiation) or through the adjoint method [7]. Several automatic differentiation codes for a variety of programming languages exist and are widely used. Prominent software packages are ADIFOR and ADI-C codes for FORTRAN and C, respectively [13,14]. Automatic differentiation is accurate because each derivative evaluation can be done symbolically, which means that the error will be due to machine round off. Automatic differentiation is also efficient for computing high-dimensional gradients. The disadvantages to automatic differentiation are that software modifications are required and the resulting new software is not easily optimized for efficiency [7].

Over the last few decades, alternative numerical differentiation techniques have emerged for use in sensitivity analysis. Two of these methods are complex Taylor series expansion (CTSE), also referred to as the complex step derivative method, and Fourier differentiation (FD). These methods are conceptually simpler to implement than direct differentiation, the adjoint method, or automatic differentiation and offer more accurate and stable derivatives compared to finite differencing.

Complex variable sensitivity methods have some potentially significant advantages over other techniques. For example, the concept is simple and analogous to finite differentiation. In this case, a reanalysis is required with a perturbation of the variable of interest along the imaginary axis for CTSE (as opposed to the real axis for finite differencing) and with perturbations along a sampling radius in the complex plane for FD. Also, implementation is straightforward using complex variable operations. A significant advantage of these methods is that they are robust to the step size used for the reanalyses, unlike finite differencing. A disadvantage of complex variable sensitivity methods is that a reanalysis is needed for each parameter of interest. Thus, these methods are likely not an efficient way to compute a large number of sensitivities.

CTSE was first described by Lyness and Moler [15,16] in the late 1960s. It reemerged as a tool for engineering analysis with a paper by Squire and Trapp in 1998 [17]. Since then it has been used in a wide variety of engineering fields including computational fluid dynamics, dynamic system optimization and many others [18–25]. In all of these applications, CTSE has offered a great improvement in accuracy over finite differencing.

FD was also developed by Lyness in the late 1960s and early 1970s [15,16,26]. The method was further described by Henrici and more recently Bagley [27,28]. The method utilizes additional sample points in the complex plane and an FFT routine to calculate derivatives (including high order) with exceptional accuracy. To date, the method has not been widely used for the determination of sensitivities for engineering problems.

The goal of this paper is to demonstrate the use of complex variable methods for the calculation of shape sensitivities using the finite element method. Two linear elastic problems with known analytical solutions are solved to demonstrate the accuracy of the complex variable sensitivity methods in comparison with exact analytical and finite differencing solutions.

2. Methodology

2.1. Numerical differentiation

Finite differencing is a well-known method to obtain an estimate of a function's derivative that is simple in concept and application. A derivative is defined as the limit (provided the limit exists) of the change in a function's value across two different points as the distance between the two points goes to zero

$$f'(x_0)=\lim_{x\to x_0}\frac{f(x)-f(x_0)}{x-x_0} \tag{1}$$

Finite differencing methods estimate derivatives by approximating the limit in Eq. (1) as a difference between a function evaluated a two distinct points located a distance h apart divided by h

$$f'(x_o)\approx\frac{f(x_o+h)-f(x_o)}{h} \tag{2}$$

This distance, h, is often called the step size. When h is positive, the method is referred to as forward differencing. When h is negative it is called backwards differencing. When the forward difference and the backwards difference results are averaged, the method is called central differencing (CD). The equation for central differencing is as follows:

$$f'(x_o)\approx\frac{f(x_o+h)-f(x_o-h)}{2h} \tag{3}$$

The required analyses in the complex plane are shown in Fig. 1. The diamonds indicate that two analyses are required around the sample point X, that is, the real value of X is perturbed

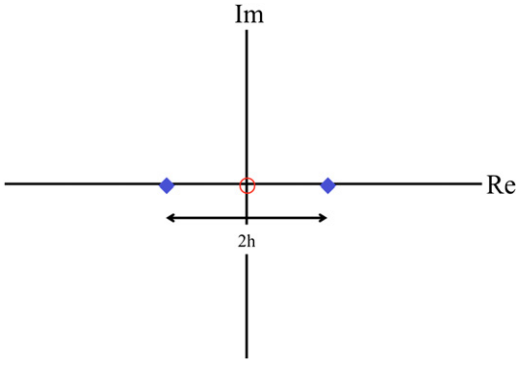

Fig. 1. Schematic of central differencing (analyses required at the diamonds).

by plus and minus h along the real axis. Finite differencing is very straightforward as no source code changes are required; the only effort is to perform multiple runs.

Although simple and often effective, the finite difference method suffers from one significant drawback. The approximation of derivatives as a difference between two nearly equal numbers leads to error due to the truncation of terms in the function's Taylor series. This error can be eliminated by making the step size as small as possible. However, as the step size is reduced a new source of error arises. This error is round-off error and it is due to the fact that a computer cannot accurately calculate a small difference between two near-equal numbers. This means that for finite differencing there is a lower limit on the step size and also a limit on the maximum achievable accuracy.

For the forward differencing method, none of the higher order terms cancel leaving an order of accuracy for a given step size of $O(h)$. Using CD, the even order terms in the Taylor series cancel and the accuracy of the method becomes $O(h^2)$.

Higher order derivatives can also be calculated through CD by using additional sample points. For example, using three analyses, the formula for the second derivative is

$$f^{(2)}(x_o) \approx \frac{f(x_o+h)-2f(x_o)+f(x_o-h)}{h^2} \tag{4}$$

where the superscript (2) denotes the second derivative.

One of the problems with CD is that the calculation of higher order derivatives requires more sample points and more difference operations. Each additional difference operation results in an increase in the round-off error, which further restricts the lower limit of h. This means that CD is not a good choice for the calculation of higher order derivatives.

Since, as described above, too large a step size poorly approximates the limiting process of the derivative, Eq. (1), and too small a step size provides an inaccurate estimate due to round-off error, it is frequently difficult to obtain an accurate estimate of the derivative using finite differencing. A costly trial-and-error approach may be required which does not generalize to other problems and other derivatives.

A related difficulty with applying finite differencing for shape sensitivity analysis in finite element methods is that a perturbation of the mesh is required to implement the step size h. This perturbation in the mesh may be difficult to implement without mesh distortion issues.

CTSE is a numerical differentiation method similar in spirit and concept to finite differencing but with significant advantages. CTSE uses the orthogonality of the real and imaginary axes of the complex plane to calculate derivatives with fewer difference operations and in turn less round-off error when compared to CD. Similar to finite differencing, CTSE requires the difference of two analyses but with a small perturbation along the imaginary axis. That is, variable $X=x_0$ is perturbed to $X=x_0+ih$, where i denotes an imaginary number and h denotes the step size, see Fig. 2. The formulae for the derivatives can be derived from the Taylor series representation of the function evaluated at the complex sample point

$$f(x_0+ih) = f(x_0)+f^{(1)}(x_0)\frac{ih}{1!}+f^{(2)}(x_0)\frac{(ih)^2}{2!}+f^{(3)}(x_0)\frac{(ih)^3}{3!}+\cdots \tag{5}$$

where $f^{(1)}$ denotes the first derivative, $f^{(2)}$ the second, etc. Taking the imaginary part of both sides of Eq. (5), solving for the first derivative and ignoring terms of $O(h^2)$ yields an estimate of the first derivative

$$f^{(1)}(x_o) \approx \frac{\mathrm{Im}(f(x_o+ih))}{h} \tag{6}$$

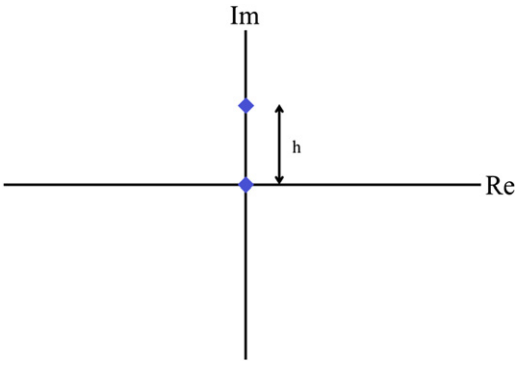

Fig. 2. Schematic of the complex Taylor series expansion (analyses required at the diamonds).

Note that no difference operation is needed for the first derivative. This means that the step size can be made arbitrarily small with no concern about round-off error.

Higher order derivatives can be computed using CTSE. Taking the real part of Eq. (5), the formula for the second derivative with error $O(h^2)$ can be derived as

$$f^{(2)}(x_o) \approx \frac{2(f(x_o)-\mathrm{Re}(f(x_o+ih)))}{h^2} \tag{7}$$

Note, however, that the second derivative contains a difference operation meaning that round-off error will be a problem if h is set too small.

By using more sample points along the imaginary axis, it is possible to solve Eq. (5) to obtain the higher order derivatives. For example, if 2 sample points are used along the imaginary axis in addition to the original sample, the real and imaginary terms of the Taylor series can be used to create a system of equations that can be solved for the desired derivatives. For example, considering 2 points along the imaginary axis in addition to the initial point,

$$\begin{aligned}
\mathrm{Im}(f(x_0+ih)) &= f^{(1)}(x_0)\frac{h}{1!}-f^{(3)}(x_0)\frac{h^3}{3!}+f^{(5)}(x_0)\frac{h^5}{5!}+\ldots\\
\mathrm{Im}(f(x_0+2ih)) &= f^{(1)}(x_0)\frac{2h}{1!}-f^{(3)}(x_0)\frac{(2h)^3}{3!}+f^{(5)}(x_0)\frac{(2h)^5}{5!}+\ldots\\
\mathrm{Re}(f(x_0+ih)) &= f(x_0)-f^{(2)}(x_0)\frac{h^2}{2!}+f^{(4)}(x_0)\frac{h^4}{4!}+\ldots\\
\mathrm{Re}(f(x_0+2ih)) &= f(x_0)-f^{(2)}(x_0)\frac{(2h)^2}{2!}+f^{(4)}(x_0)\frac{(2h)^4}{4!}+\ldots
\end{aligned} \tag{8}$$

Solving the system of equations yields the first four derivatives

$$\begin{aligned}
f^{(1)}(x_0) &\approx \frac{\frac{4}{3}\mathrm{Im}(f(x_0+ih)-\frac{1}{6}\mathrm{Im}(f(x_0+2ih))}{h}\\
f^{(2)}(x_0) &\approx \frac{\frac{9}{4}f(x_0)-\frac{7}{3}\mathrm{Re}(f(x_0+ih)-\frac{1}{12}\mathrm{Re}(f(x_0+2ih))}{h^2}\\
f^{(3)}(x_0) &\approx \frac{2\mathrm{Im}(f(x_0+ih)-\mathrm{Im}(f(x_0+2ih))}{h^3}\\
f^{(4)}(x_0) &\approx \frac{6f(x_0)-4\mathrm{Re}(f(x_0+ih)+2\mathrm{Re}(f(x_0+2ih))}{h^4}
\end{aligned} \tag{9}$$

However, the quality of the derivatives using this approach will depend on the step size h.

FD is a superior method for obtaining higher order derivatives [28]. The heart of FD is making a real valued function become a periodic complex function. This is accomplished by adding a periodic, oscillatory, complex component to each of the function's real independent variables. The resulting periodic function now has a Taylor series representation that takes on the properties of a periodic Fourier series. Fast Fourier transform techniques are used to determine the coefficients of this series. The resulting coefficients contain the function's derivatives.

A central feature of Fourier differentiation is to make the individual terms in the Taylor series oscillate at different frequencies. To achieve these oscillations, the perturbation to the variable x is taken to be a complex number as $\Delta x = ce^{-i\theta}$, where c is a sampling radius. This expression extracts from the series the nth coefficient that contains the nth derivative of the function

$$\frac{1}{2\pi}\int_{-\infty}^{\infty} f(x_o + ce^{-i\theta})e^{in\theta}\,d\theta = \frac{f^{(n)}(x_0)c^n}{n!} \tag{10}$$

Although Fourier differentiation appears more complex than CTSE, operationally it is similar in that multiple analyses are required in the complex plane evaluated at N sample points along a circular contour c in the complex plane centered on the initial point, see Fig. 3. The vector of the output data is run through an FFT routine and the output is the first N terms in the function's Taylor series. The nth order derivative of the function can then be calculated from the Taylor series coefficients by using the following relationship

$$f^{(n)}(z_o) = \frac{a_n n!}{c^n} \tag{11}$$

where a_n is the nth Taylor series coefficient. Note, however, that Fourier differentiation requires samples in the real and imaginary plane, thus, perturbations of the finite element mesh in the real and imaginary domains are necessary whereas CTSE only requires perturbations of the finite element mesh along the imaginary axis.

2.2. Finite element implementation

CTSE and FD are implemented in the finite element method through the concept of complex valued nodal coordinates. This concept is outlined through a simple one-element cantilever beam analysis below where the sensitivity with respect to beam length is computed.

Consider a horizontal cantilevered beam with a point load applied at the free end with properties: E—modulus of elasticity, I—cross-sectional moment of inertia, P—force applied at the free end, L—length, with vertical displacement δ and rotation ϕ, see Fig. 4.

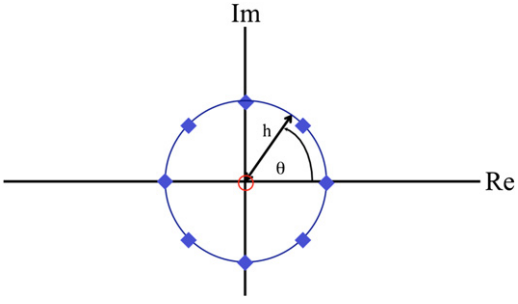

Fig. 3. Schematic of analyses required for Fourier differentiation (analyses required at the diamonds).

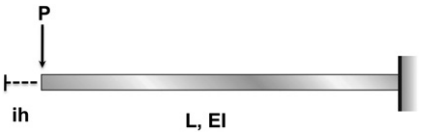

Fig. 4. Cantilever beam with imaginary increment in length.

The system of equations for a single element after fixing the displacement and rotation of the right end is

$$\begin{Bmatrix} P \\ 0 \end{Bmatrix} = \frac{EI}{L^3}\begin{bmatrix} 12 & 6L \\ 6L & 4L^2 \end{bmatrix}\begin{Bmatrix} \delta \\ \phi \end{Bmatrix} \tag{12}$$

The sensitivity with respect to the length of the beam can be obtained by perturbing the element length in the imaginary domain by a small step h, i.e., $L+ih$. In general, this would be done by perturbing the nodal coordinates in the imaginary domain. The resulting stiffness matrix is now complex and the system of equations becomes

$$\begin{Bmatrix} P \\ 0 \end{Bmatrix} = \frac{EI}{(L+ih)^3}\begin{bmatrix} 12 & 6(L+ih) \\ 6(L+ih) & 4(L+ih)^2 \end{bmatrix}\begin{Bmatrix} \delta \\ \phi \end{Bmatrix} \tag{13}$$

Solution of the system of equations yields

$$\begin{Bmatrix} \delta \\ \phi \end{Bmatrix} = \frac{P(L+ih)^2}{6EI}\begin{Bmatrix} 2(L+ih) \\ -3 \end{Bmatrix} \tag{14}$$

Expanding δ

$$\delta = \left\{\frac{PL^3}{3EI} - \frac{PLh^2}{EI}\right\} + i\left\{\frac{PL^2h}{EI} - \frac{Ph^3}{3EI}\right\} \tag{15}$$

The displacement is obtained from Re[δ] as

$$\delta = \left\{\frac{PL^3}{3EI} - \frac{PL}{EI}h^2\right\} \tag{16}$$

Note that the displacement is exact up to $O(h^2)$. Since the derivative can be obtained without subtracting two near-equal numbers, h can be made as small as desired and the exact solution for the displacement (and rotation) is recovered numerically.

The derivative of the displacement with respect to beam length is determined from

$$\frac{\partial\delta}{\partial L} = \mathrm{Im}[\delta]/h = \left\{\frac{PL^2}{EI} - \frac{P}{3EI}h^2\right\} \tag{17}$$

The derivative is exact up to $O(h^2)$ and the exact solution is recovered numerically as h is reduced. The significant advantage of CTSE over finite differentiation is that the selection of the step size h is largely a non-issue since very small values can be used. In addition, for small values of h, the traditional results from the finite element solution (in this case displacement and rotation) are effectively unchanged.

In this example, the shape sensitivity involved perturbing the X coordinate of the node at the end of the beam as $X+ih$. Note, however, that any arbitrary perturbation to the shape of the beam can be affected by perturbing the X and Y coordinates in the imaginary domain for 2D problems and perturbing the X, Y, and Z coordinates for 3D problems. That is, the X, Y, and Z coordinates of the imaginary step can be adjusted to configure whatever shape sensitivity is desired. For example, the sensitivity with respect to the curvature of a beam can be assessed by perturbing the Y coordinates along the beam according to the desired curved shape; or the shape sensitivity with respect to a hole's radius can be determined by implementing a radial perturbation of the imaginary components of the nodes on the edge of the hole.

It is significant to note that perturbing the mesh in the imaginary domain is a mathematical operation and avoids the tediousness of remeshing and mesh distortion issues.

While CTSE is simple in concept and analogous to finite differentiation, it requires the finite element software be written to systemically handle complex variables, i.e., the stiffness matrix will be complex, the solver must invert a complex matrix, etc. However, no additional derivation or programming of equations is required such as when implementing direct differentiation or the adjoint method. Also, the introduction of complex variable

nodal coordinates causes a systemic change to the results. All results such as displacements, temperatures, velocities, strains, stresses etc. are complex. Although, we have demonstrated the method for shape sensitivities, sensitivities with respect to other properties can be obtained using complex variable sensitivity method such as with respect to loading or material properties.

A two-dimensional finite element code capable of solving the 2-D equations of elasticity under the assumptions of plane stress was written in Matlab. The code used second order shape functions and six-node triangular elements. The equations for the shape functions in terms of the natural coordinates can be found in Huebner [30]. Geometry and meshes were created using the Comsol finite element package and were then imported into Matlab. After importation, the edges of the elements were reconstructed so that all element edges were linear, and all non-vertex nodes were placed on the midpoint of the edges. The use of natural coordinates and straight edged elements allowed the stiffness matrix to be computed algebraically. The code used a conjugate gradient solver with a minimum error of 1E−8. After solving the global system of equations for the displacements, the stresses at each of the nodes were calculated on an element-by-element basis using the equations of elasticity, second order shape functions and the nodal displacements. Since, the nodal stress calculated from one element does not always agree with the nodal stress calculated using another element, stress averaging was used to smooth the stress field at nodal points. The code then calculated the principal stresses and the Von Mises stresses using the stresses at the nodal points.

In order to perform the shape sensitivity calculations, a small step must be added to the affected nodal coordinates. This was done by first identifying the nodes located on the geometry feature being sampled. The code then added a small step (real—CD, imaginary—CTSE, or both—FD, depending on the method) to the nodal coordinate of each of the affected nodes. The relative perturbation of the X and Y coordinates depended upon the sensitivity being computed. All other nodes in the model remained the same. If the step size chosen for the numerical differentiation technique is very large, be it real or imaginary, the elements may become distorted, which can lead to poor numerical results. As such, the step sizes and sampling radii were typically kept much smaller than the edge lengths of the affected elements.

3. Numerical example: thick walled cylinder

In order to test the accuracy of the three numerical differentiation techniques two problems with an analytical solution were solved. The first problem was the thick walled cylinder under uniform boundary pressure. The equations that govern the stress through the thickness of the cylinder are given in [29]

$$\sigma_r = \frac{r_1^2 r_2^2 p}{r_2^2 - r_1^2}\frac{1}{r^2} - \frac{r_2^2 p}{r_2^2 - r_1^2}$$
$$\sigma_\theta = \frac{r_1^2 r_2^2 p}{r_2^2 - r_1^2}\frac{1}{r^2} - \frac{r_2^2 p}{r_2^2 - r_1^2} \quad (18)$$

where r_1 is the inner radius, r_2 is the outer radius, and p is the boundary pressure. For this example, the inner radius of the cylinder was 0.5 m, the outer radius was 1 m, and the boundary pressure was 10 kPa. The stress equations given in Eq. (18) were differentiated with respect to the inner radius to generate the

Table 1
The L_2 error norm in the stress solutions for a thick walled cylinder.

Number of elements	Radial stress	Tangential stress
888	6.257E−3	3.551E−3
1792	3.347E−3	2.009E−3
6184	9.715E−4	7.280E−4
25,124	2.682E−4	3.343E−4

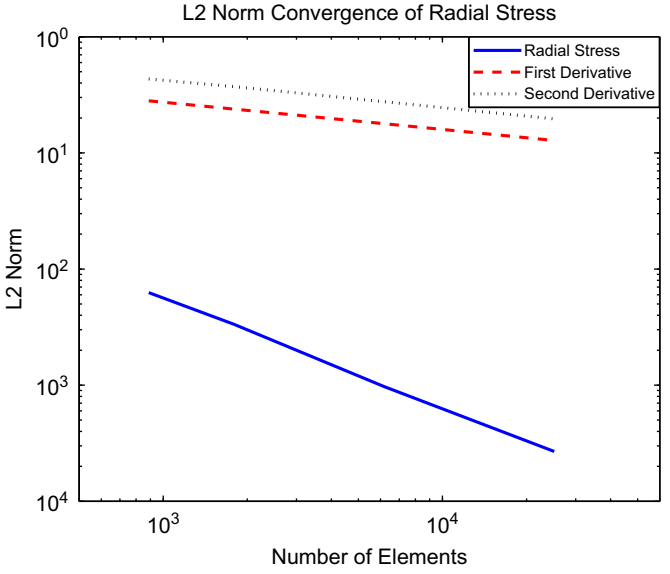

Fig. 6. Convergence of the L_2 norm for the radial stress and the first two sensitivities for the thick walled cylinder.

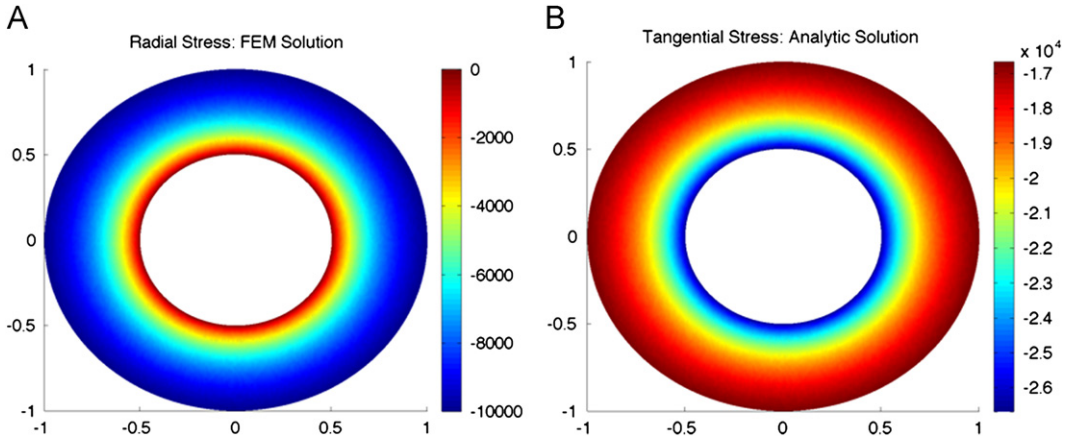

Fig. 5. The numerical solution of the radial and tangential stresses for the radial stress of a thick walled cylinder. (A) The FEM solution for the radial stresses. (B) The FEM solution for the tangential stresses.

sensitivities of the stresses. The first and second order sensitivities of the stresses with respect to the inner radius are given in Eqs. (19) and (20), respectively

$$\frac{\partial \sigma_r}{\partial r_1} = 2\left[\frac{r_1 {r_2}^2 p}{({r_2}^2 - {r_1}^2)^2}\left(\frac{{r_2}^2}{r^2} - 1\right)\right]$$
$$\frac{\partial \sigma_\theta}{\partial r_1} = -2\left[\frac{r_1 {r_2}^2 p}{({r_2}^2 - {r_1}^2)^2}\left(\frac{{r_2}^2}{r^2} + 1\right)\right] \quad (19)$$

$$\frac{\partial^2 \sigma_r}{\partial {r_1}^2} = 2\left[\frac{(3r_1^2 + r_2^2) {r_2}^2 p}{({r_2}^2 - {r_1}^2)^3}\left(\frac{{r_2}^2}{r^2} - 1\right)\right]$$
$$\frac{\partial^2 \sigma_\theta}{\partial {r_1}^2} = -2\left[\frac{(3r_1^2 + r_2^2) {r_2}^2 p}{({r_2}^2 - {r_1}^2)^3}\left(\frac{{r_2}^2}{r^2} + 1\right)\right] \quad (20)$$

Table 2
The computational time required to solve each model for a thick walled cylinder.

Number of elements	Compute time (s)
888	8.49
1792	19.48
6184	130.8
25,124	2799

Table 3
The L_2 norm of the error in the first second and third order sensitivities of the stress to the inner radius for a thick walled cylinder (6184-element model).

Method	Radial stress			Tangential stress		
Order	1st	2nd	3rd	1st	2nd	3rd
CD	1.786E−1	2.763E−1	1.558E0	7.026E−2	1.007E−1	3.818E−1
CTSE	1.786E−1	2.762E−1	1.540E0	7.026E−2	1.007E−1	3.796E−1
FD	1.786E−1	2.762E−1	1.576E0	7.026E−2	1.007E−1	3.837E−1

The problem was solved using four different meshes in order to examine the convergence of the error in the sensitivities. The coarsest mesh contained 888 elements, and 1868 nodes; the next mesh contained 1792 elements and 3716 nodes; the third mesh contained 6184 elements and 12,608 nodes; and the finest mesh consisted of 25,124 elements and 50,724 nodes. The solutions for the radial and tangential stresses as calculated using the 6184-element mesh are shown in Fig. 5.

The normalized L_2 norm was selected in order to compare the error in the four different mesh cases

$$||norm||_{L_2} = \frac{(\int (\sigma_{analytical} - \sigma_{numerical})^2 dA)^{1/2}}{(\int (\sigma_{analytical})^2 dA)^{1/2}} \quad (21)$$

Integration was performed using fifth order Gaussian quadrature. All figures for this example display the L_2 norm per element normalized by the L_2 norm integrated over the entire model. Table 1 shows the norm of the error in both the radial and tangential stress solutions for each mesh case. This data is shown graphically in Fig. 6 on a log–log plot (solid line). It is seen that the slope of the norm in log–log space is approximately -1.

The amount of computational time (wall time) needed to solve a real valued solution for each mesh case is shown in Table 2. Given the amount of computational time required for 25,124 element case and the fact that the complex sensitivity solutions require three times more computation than the real valued case, the 6184 element case was used for the figures and to compare the sensitivity results obtained using different sampling radii and step sizes. For each sensitivity method, unless otherwise noted, the step size (h) or sampling radius (c) was 0.001, which was approximately 1/30th of the average element edge length. CTSE was performed using two sample points for all sensitivities, and FD was performed using 6 sample points. CD used 2 points to estimate the 1st derivative, 3 points to estimate the 2nd derivative, and 4 points to estimate the 3rd derivatives.

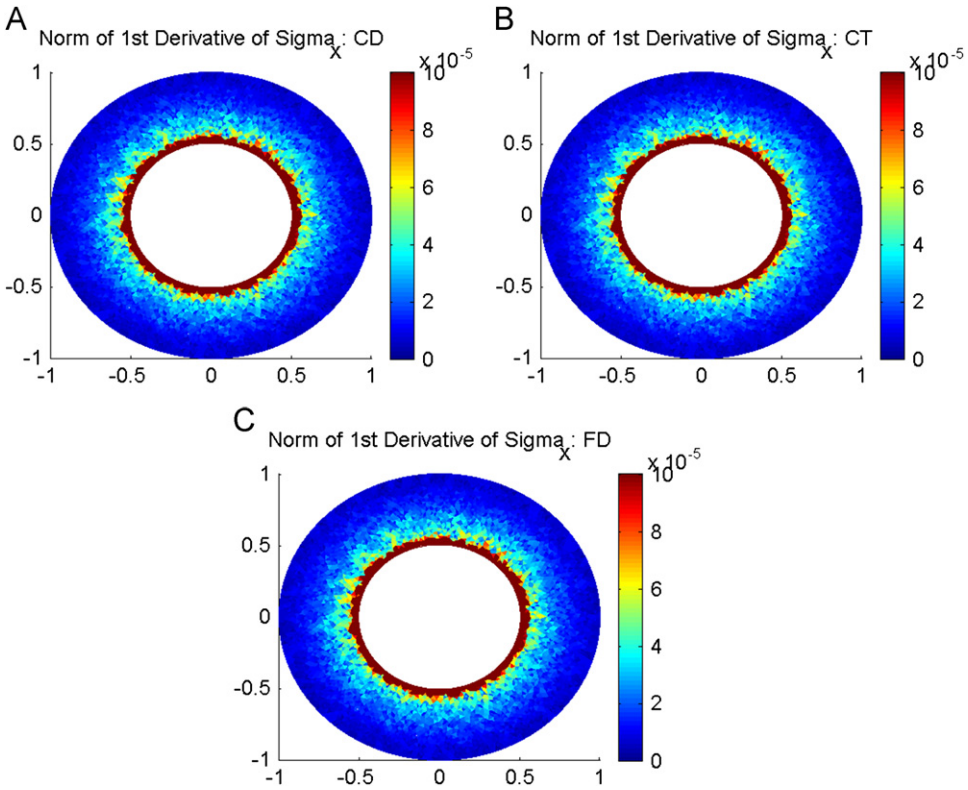

Fig. 7. The L_2 norm of the error in the first order sensitivity of the radial stress of a thick walled cylinder. (A) Error in CD, (B) error in CTSE, (C) error in FD.

The L_2 norm of the error in the sensitivities appears in Table 3 and is shown graphically in Fig. 6 for the various meshes. The norm of the error in the first order sensitivities of the radial stress over the domain appears in Fig. 7, and the norm for the second order sensitivities appears in Fig. 8 for the 6184 element mesh. These figures show only very slight differences between the three methods.

The norm of the error in each case is mostly independent of the method selected. The third order sensitivities show some small differences between the methods (see Table 3), with CTSE having the highest accuracy. The fact that the error is similar between all three methods points to the fact that the error in the finite element solution is dominating errors arising from the differentiation methods themselves. This is seen by looking at the first and second order sensitivities of the radial stress as a function of the number of elements shown in Table 4. It is seen that each additional mesh refinement increases the accuracy of the method and it is clear that the changes due to mesh convergence are much greater than any differences between the methods.

The errors in the first and second order sensitivities of the radial stress calculated using three different step sizes are shown in Table 5. It is seen that changing the step size does not have much effect on the accuracy of the sensitivity. This is a further indicator that the accuracy of the finite element solution is limiting the accuracy of the sensitivities, not the accuracy of the numerical differentiation methods. One exception is the second order sensitivity at the smallest step size, 0.0001 or 1/300th of the average element edge length. At this step size each method produces sensitivities that are less accurate than those calculated with a larger step size. This indicates that the machine round-off error associated with this step size may be approaching the magnitude of the error in the finite element solution.

4. Numerical example: disk in diametrical compression

One of the classical tests in material analysis is the disk in diametrical compression [29]. In this test, a circular disk is loaded in compression along its y-axis. The load is modeled as a point load. This loading and geometry generates a uniform tensile stress along the x-axis of the specimen. It is thus useful in examining the tensile properties of a material without actually loading the specimen in tension. This test is also known as the indirect tensile test or the Brazil nut test.

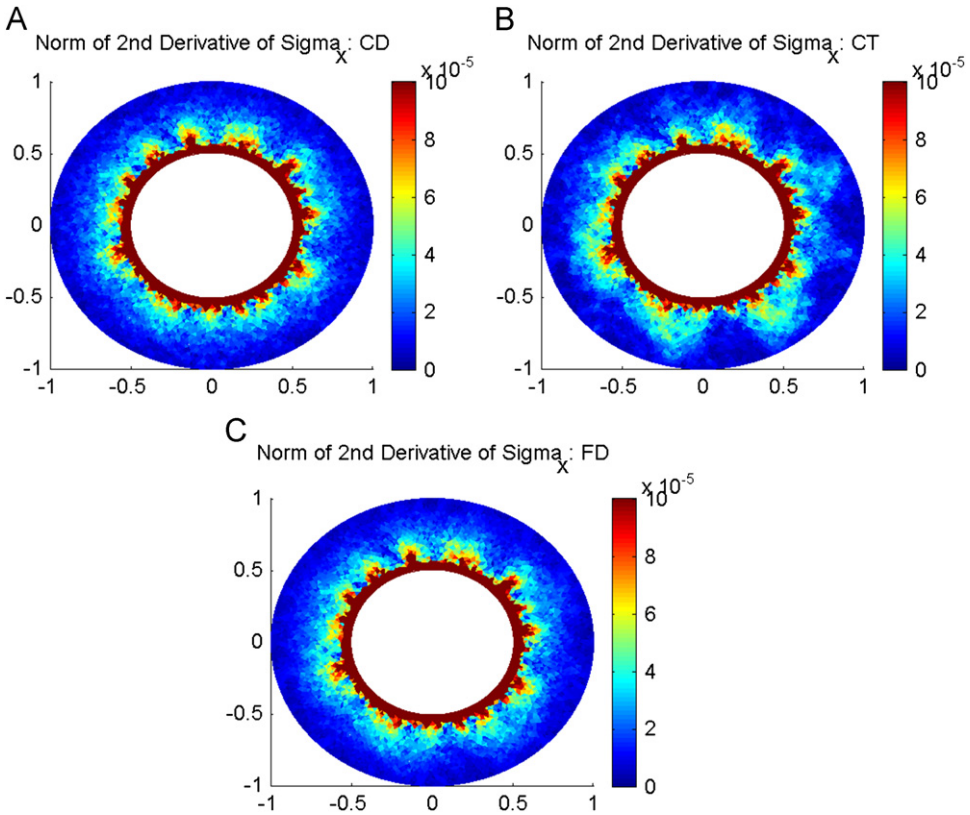

Fig. 8. The L_2 norm of the error in the second order sensitivity of the radial stress to the inner radius of a thick walled cylinder. (A) Error in CD, (B) error in CTSE, (C) error in FD.

Table 4
The L_2 norm of the error in the first and second order sensitivities of the radial stress as a function of the number of elements for a thick walled cylinder.

Number of elements	CD		CTSE		FD	
Order	1st	2nd	1st	2nd	1st	2nd
888	2.806E−1	4.339E−1	2.805E−1	4.327E−1	2.806E−1	4.331E−1
1792	2.387E−1	3.769E−1	2.386E−1	3.728E−1	2.386E−1	3.742E−1
6184	1.786E−1	2.763E−1	1.786E−1	2.762E−1	1.786E−1	2.762E−1
25,124	1.280E−1	1.963E−1	1.280E−1	1.963E−1	1.280E−1	1.963E−1

The diametrical compression test has an analytical solution that can be derived through superposition. The solution for the stresses is shown in [29]

$$\sigma_x = \frac{-2P}{\pi}\left[\frac{(R-y)x^2}{(x^2+(R-y)^2)^2}+\frac{(R+y)x^2}{(x^2+(R+y)^2)^2}-\frac{1}{2R}\right]$$

$$\sigma_y = \frac{-2P}{\pi}\left[\frac{(R-y)^3}{(x^2+(R-y)^2)^2}+\frac{(R+y)^3}{(x^2+(R+y)^2)^2}-\frac{1}{2R}\right]$$

$$\tau_{xy} = \frac{2P}{\pi}\left[\frac{(R-y)^2x}{(x^2+(R-y)^2)^2}+\frac{(R+y)^2x}{(x^2+(R+y)^2)^2}\right] \quad (22)$$

In these equations, P is the magnitude of the point load, R is the radius of the disk, and x and y specify the location at which the stress is calculated, with the point (0,0) located at the center of the disk. The analytic solutions of Eq. (22) can be differentiated to yield the sensitivities with respect to the radius of the disk. The equations for the first two sensitivities of the normal stress in the x-direction with respect to the radius are

$$\frac{d\sigma_x}{dR} = \frac{2P}{\pi}\left[\frac{(3R^2-6Ry-x^2+3y^2)x^2}{(x^2+(R-y)^2)^3}+\frac{(3R^2+6Ry-x^2+3y^2)x^2}{(x^2+(R+y)^2)^3}+\frac{1}{2R^2}\right]$$

$$\frac{d^2\sigma_x}{dR^2} = \frac{-2P}{\pi}\left[\frac{12(R-y)(R^2-2Ry-x^2+y^2)x^2}{(R^2-2Ry+x^2+y^2)^4}+\frac{12(R+y)(R^2+2Ry-x^2+y^2)x^2}{(R^2+2Ry+x^2+y^2)^4}-\frac{1}{R^3}\right] \quad (23)$$

The diametrical compression test model was solved using three different meshes; a coarse mesh consisting of 1148 elements and 2357 nodes; a moderately refined mesh of 2502 elements and 5093 nodes; and a fine mesh with 8374 elements and 16,909

Table 6
The L_2 norm of the error in the stress solutions for a disk under diametrical compression.

Number of elements	Norm of error in stress in X	Norm of error in stress in Y	Norm of error in shear stress
1148	7.993E−2	5.002E−2	9.324E−2
2502	3.454E−2	1.108E−2	2.194E−2
8374	1.013E−2	3.239E−3	7.396E−3

Table 5
The L_2 norm of the error in the first and second order sensitivities of the radial stress as a function of step size for a thick walled cylinder.

Step size	CD		CTSE		FD	
Order	1st	2nd	1st	2nd	1st	2nd
0.0001	1.786E−1	2.764E−1	1.786E−1	2.817E−1	1.786E−1	2.763E−1
0.001	1.786E−1	2.763E−1	1.786E−1	2.762E−1	1.786E−1	2.762E−1
0.01	1.788E−1	2.841E−1	1.786E−1	2.731E−1	1.786E−1	2.766E−1

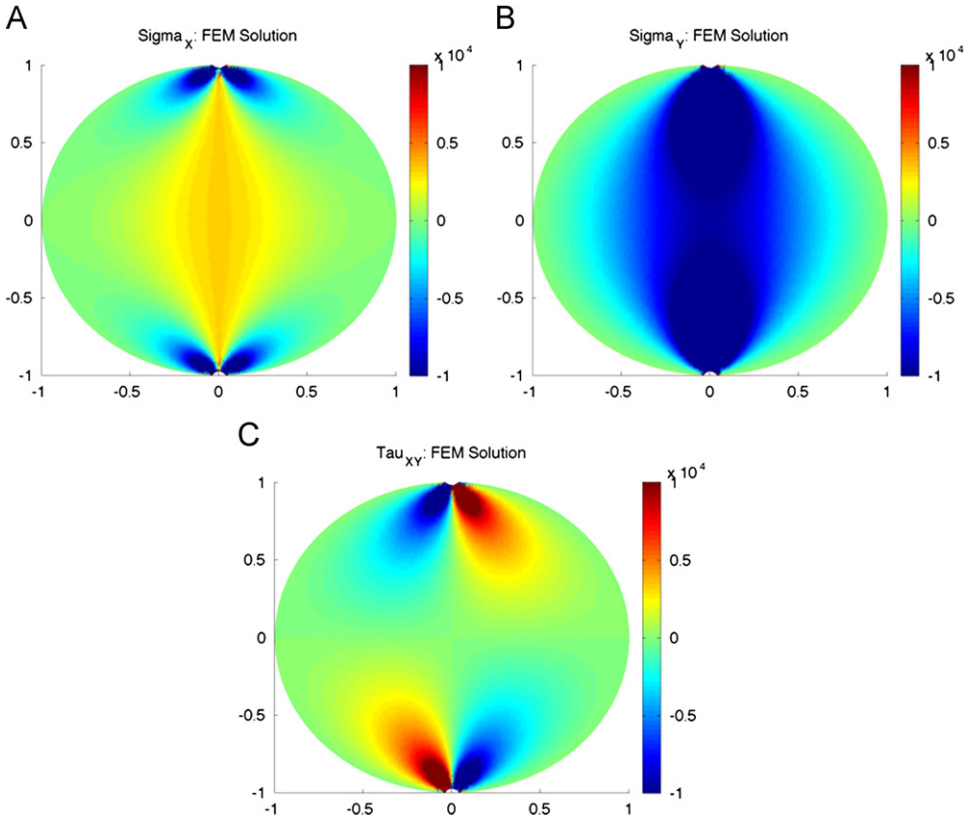

Fig. 9. The finite element solution for the stresses in a disk in diametrical compression. (A) Normal stress in the x-direction. (B) Normal stress in the y-direction. (C) Shear stress.

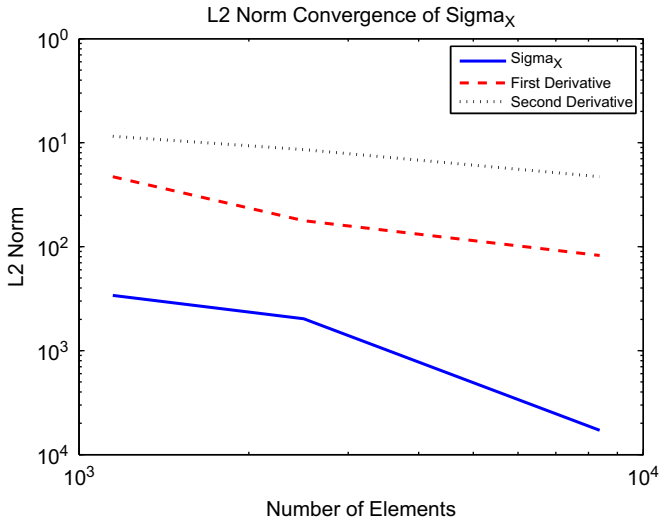

Fig. 10. Convergence of the L_2 norm for the stress in the x-direction and the first two sensitivities for a disk in diametrical compression.

Table 7
The computational time required to solve each model for a disk under diametrical compression.

Number of elements	Compute time (s)
1148	10.41
2502	27.82
8374	200.0

nodes. The solution for the stresses as calculated using the fine mesh appears in Fig. 9. It should be noted that for each figure in this example, no solution is plotted for the elements near where the load is applied due to the stress concentration of the point load. For all norms discussed in this problem, the contributions of any element with a node within 10% of the radius from the load were neglected. The L_2 norm shown in Eq. (21) was used.

Table 6 shows the norm for the three stresses for the three different mesh sizes. As for the thick walled cylinder, it is seen that each successive mesh refinement results in a significant reduction in the error norm. The norm of the normal stress in the x-direction and the first two sensitivities versus the number of elements is shown visually on a log–log scale in Fig. 10. As the number of elements increases, the error norm with respect to σ_x decreases with a slope of about 1.5. The computational time required to generate one real-valued solution appears in Table 7.

The L_2 error norm of the first and second order sensitivities of the normal stress in the x-direction with respect to the disk radius are shown in Fig. 11 (first order) and Fig. 12 (second order) for the fine mesh case. It is clear that the methods produce consistent results. As for the thick walled cylinder, the first and second order derivatives exhibit higher error along the circumference of the disk. It is also noted that there is higher error near the loading points due to the high stress concentration from the point load.

The norm of the error in the first and second order sensitivities is shown in Table 8. Again it is seen that the error is highly dependent on the number of elements, but not very dependent on the solution method. This points to the fact that the error in the derivatives is not due to the truncation error of the derivative methods, since the truncation error of CD is of the order $O(h^2)$, CTSE is of the order $O(h^4)$ while the truncation error of FD is $O(h^6)$. The lack of dependence on the choice of method is further shown

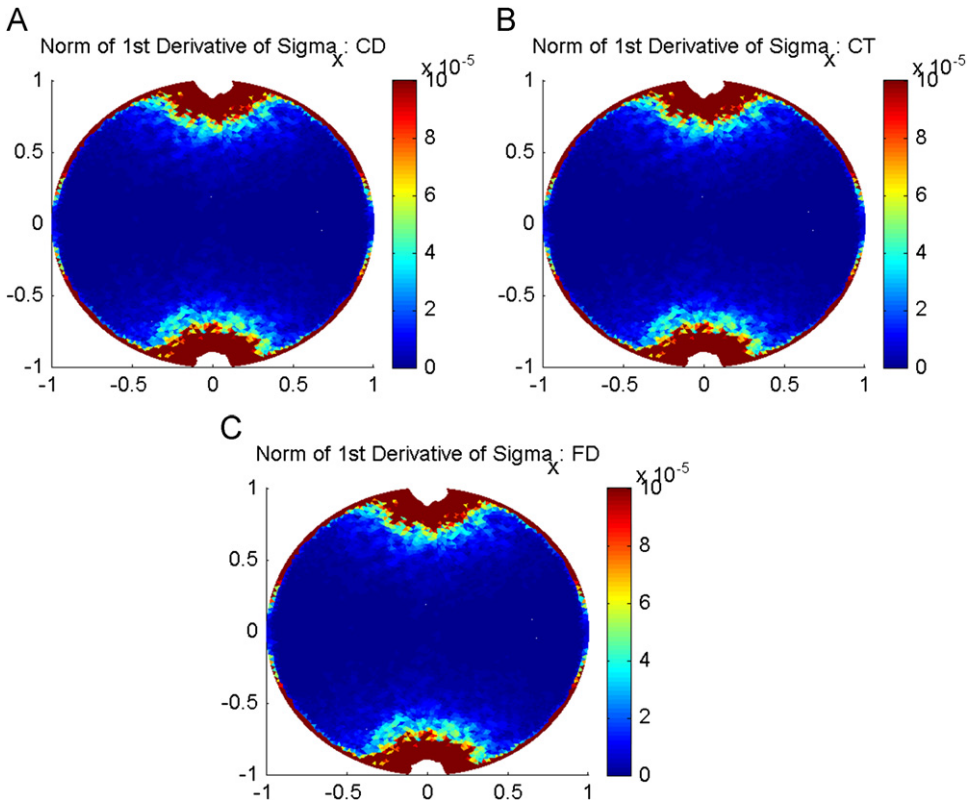

Fig. 11. The norm of the error in the first order sensitivity for a disk under diametrical compression. (A) Solution calculated by CD. (B) Solution calculated by CTSE. (C) Solution calculated by FD.

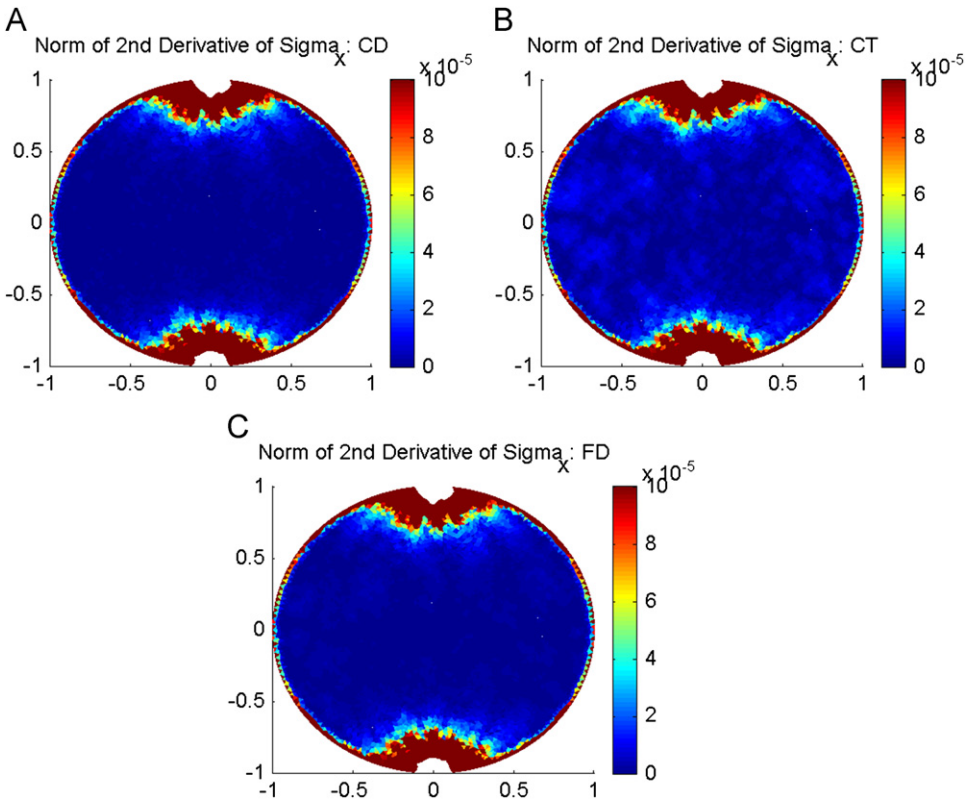

Fig. 12. The norm of the error in the second order sensitivity for a disk under diametrical compression. (A) Solution calculated by CD. (B) Solution calculated by CTSE. (C) Solution calculated by FD.

Table 8
The L_2 norm of the error in the first and second order sensitivities of the normal stress in the x-direction as a function of the number of elements for a disk under diametrical compression.

Number of elements\order	CD		CTSE		FD	
	1st	2nd	1st	2nd	1st	2nd
1148	5.338E−1	4.774E−1	5.338E−1	4.774E−1	5.338E−1	4.774E−1
2502	3.301E−1	2.869E−1	3.301E−1	2.870E−1	3.301E−1	2.870E−1
8374	2.445E−1	1.209E−1	2.444E−1	1.210E−1	2.444E−1	1.210E−1

Table 9
The L_2 norm of the error in the first and second order sensitivities of the radial stress as a function of step size for a disk under diametrical compression (8374-element mesh).

Step size	CD		CTSE		FD	
Order	1st	2nd	1st	2nd	1st	2nd
0.0001	2.444E−1	1.210E−1	2.444E−1	1.264E−1	2.444E−1	1.214E−1
0.001	2.445E−1	1.209E−1	2.444E−1	1.210E−1	2.444E−1	1.210E−1
0.01	2.457E−1	1.151E−1	2.448E−1	1.248E−1	2.445E−1	1.209E−1

in Table 9 where the norm of the errors is shown for the 8734-element mesh for three different step sizes, or sampling radii. Very little variation in the error is seen as a function of the step size (less than 1%), which is not the behavior of truncation error.

5. Conclusions

Complex variable sensitivity methods offer some advantages over other sensitivity methods. Primarily, these methods are accurate, simple in concept, largely step size independent, and do not require the derivation and implementation of additional equations such as required by direct differentiation, automatic differentiation or the adjoint method. CTSE obtains first order sensitivity information by perturbing the mesh along the imaginary axes then taking the imaginary component of the finite element output. Unlike finite differencing, no subtraction of near-equal numbers is required and the step size can be made as small as desired. By perturbing the mesh only in the imaginary domain, CTSE avoids remeshing and mesh distortion issues. This is a significant simplification over finite differencing.

FD is effective for obtaining higher order sensitivities, including mixed partial derivatives. FD requires perturbations within a sampling radius in the complex plane. The finite element outputs are then post-processed with an FFT algorithm to obtain the derivatives. CTSE can also be used to compute higher order derivatives using multiple analyses along the imaginary axis; however, the formulas require differencing operations, hence, the step size issue must be addressed. FD, like CTSE, is robust with respect to the sampling radius used for the perturbations. Therefore, the oftentimes delicate aspect of selecting a perturbation size is largely eliminated.

Complex variable sensitivity methods require the systemic change of the finite element software to be complex variable based. However, this may require few changes and frequently the modification is easily carried out. The analysis time for a complex finite element code relative to a traditional real-valued code is increased with many authors reporting a factor of approximately three [5,31].

Complex variable sensitivity methods require reanalyses for each sensitivity of interest. Therefore, they may not be a method of choice for problems requiring sensitivities with respect to a large number of parameters. However, since the entire finite element output now becomes complex, the sensitivities of all outputs with respect to the parameter of interest become available.

Several solid mechanics linear elastic solutions were demonstrated for which analytical solutions to the stress fields and the derivatives of the stresses with respect to the geometric radius were available. The results indicated that CD, CTSE, and FD all produced accurate sensitivities, although CD required a careful selection of the perturbation size. The results indicated that the accuracy of the derivatives was controlled by the accuracy of the finite element mesh. Hence, more accurate derivatives can be obtained through mesh refinement.

Acknowledgments

This work was supported under Air Force Agreement FA8650-07-C-5060, Dr. Patrick J. Golden, AFRL/RXLMN, Project Monitor.

References

[1] R.D. Cook, D.S. Malkus, M.E. Plesha, R.J. Witt, Concepts and Applications of Finite Element Analysis, John Wiley and Sons, New York, 2002.
[2] J.S. Hansen, Z.S. Liu, N. Olhoff, Shape sensitivity analysis using a fixed basis function finite element approach, Structural Multidisciplinary Optimization 21 (2000) 177–195.
[3] H.O. Madsen, L. Krenk, N.C. Lind, Methods of Structural Safety, Dover Publications, 2006.
[4] J.H. Choi, Shape design sensitivity analysis and optimization of general plane arch structures, Finite Elements in Analysis and Design 39 (2002) 119–136.
[5] J.R.R.A. Martins, P. Sturdza, J.J. Alonso, The complex-step derivative approximation, ACM Transactions on Mathematical Software 29 (2003) 245–263.
[6] R.M. Reddy, B.N. Rao, Fractal finite element method based shape sensitivity analysis of mixed-mode fracture, Finite Elements in Analysis and Design 44 (2008) 875–888.
[7] M.L.J. Rightley, R.J. Henninger, K.M. Hanson, Adjoint Differentiation of Hydrodynamic Codes, CNLS Research Highlights, Los Alamos National Laboratory, 1998.
[8] K.K. Choi, N.H. Kim, Structural Sensitivity Analysis and Optimization: Linear Systems, Volume 1, Springer Science+Business Media, 2005.
[9] Haakus and Der Kiureghian, Parameter sensitivity and importance measures in nonlinear finite element reliability analysis, Journal of Engineering Mechanics (2005) 1013–1026.
[10] C.J. Chen, K.K. Choi, Continuum approach for second-order shape design sensitivity of three-dimensional elastic solids, AIAA Journal 32 (1994) 2099–2107.
[11] A. Bebamzadeh, T. Haukaas, Second-order sensitivities of inelastic finite element response by direct differentiation, ASCE Journal of Engineering Mechanics 134 (2008) 867–880.
[12] M. Martinelli, Sensitivity Evaluation in Aerodynamic Optimal Design, Ph.D. Thesis, Scuola Normale Superiore di Pisa, 2007.
[13] C.H. Bischof, L. Roh, A.J. Mauer-Oats, ADIC: an extensible automatic differentiation tool for ANSI-C, Software-Practice and Experience 27 (1997) 1427–1456.
[14] C. Bischof, P. Khademi, A. Mauer, A. Carle, Adifor 2.0: automatic differentiation of Fortran 77 programs, IEEE Computational Science and Engineering 3 (1996) 18–32.
[15] J.N. Lyness, C.B. Moler, Numerical differentiation of analytic functions, SIAM Journal of Numerical Analysis 4 (1967) 202–210.
[16] J.N. Lyness, Differentiation formulas for analytic functions, Mathematics of Computation 22 (1968) 352–362.
[17] W. Squire, G. Trapp, Using complex variables to estimate derivatives of real functions, SIAM Review 40 (1998) 110–112.
[18] W.K. Anderson, J.C. Newman, D.L. Whitfield, E.J. Nielsen, Sensitivity analysis for Navier-Stokes equations on unstructured meshes using complex variables, AIAA Journal 39 (2001) 56–63.
[19] J.C. Newman, D.L. Whitfield, W.K. Anderson, W.K. Step-size, independent approach for multidisciplinary sensitivity analysis, Journal of Aircraft 40 (2003) 566–573.
[20] C.O.E. Burg, J.C. Newman, Computationally efficient, numerically exact design space derivatives via the complex Taylor's series expansion method, Computers and Fluids 32 (2003) 373–383.
[21] L.I. Cervino, T.R. Bewley, On the extension of the complex-step derivative technique to pseudospectral algorithms, Journal of Computational Physics 187 (2003) 544–549.
[22] X.W. Gao, M.C. He, A new inverse analysis for multi-region heat conduction BEM using complex-variable-differentiation method, Engineering Analysis with Boundary Elements 29 (2005) 788–795.
[23] J. Kim, D.G. Bates, I. Postlethwaite, Nonlinear robust performance analysis using complex-step gradient approximation, Automatica 42 (2006) 177–182.
[24] B.P. Wang, A.P. Apte, Complex variable method for eigensolution sensitivity analysis, AIAA Journal. 44 (2006) 2958–2961.
[25] N. Butuk, J.P. Pemba, computing CHEMKIN sensitivities using complex variables, Transactions of the ASME 125 (2003) 854–858.
[26] J.N. Lyness, G. Sande, ENTCAF and ENTCRE: evaluation of normalized Taylor coefficients of an analytic function, Communications of the ACM 14 (1971) 669–675.
[27] P. Henrici, Fast Fourier methods in computational complex analysis, SIAM Review 4 (1979) 481–527.
[28] R.L. Bagley, On Fourier differentiation—a numerical tool for implicit functions, International Journal of Applied Mathematics 19 (2006) 255–281.
[29] M.H. Sadd, Elasticity: Theory and Applications and Numerics, Elsevier, New York, 2005.
[30] K.H. Huebner, D.L. Dewhirst, D.E. Smith, T.G. Byrom, The Finite Element Method for Engineers, John Wiley and Sons, New York, 2001.
[31] J.C. Newman, D.L. Whitfield, W.K. Anderson, Step-size independent approach for multidisciplinary sensitivity analysis, Journal of Aircraft 40 (2003) 566–573.